The dynamic mechanism of a moving Crookes radiometer

Songze Chen, Kun Xu, and Cunbiao Lee

Citation: Phys. Fluids **24**, 111701 (2012); doi: 10.1063/1.4765353
View online: http://dx.doi.org/10.1063/1.4765353
View Table of Contents: http://pof.aip.org/resource/1/PHFLE6/v24/i11
Published by the American Institute of Physics.

The dynamic mechanism of a moving Crookes radiometer

Songze Chen,[1] Kun Xu,[2,1] and Cunbiao Lee[1,a)]
[1]*State Key Laboratory for Turbulence and Complex System, College of Engineering, Peking University, Beijing, 100871, China*
[2]*Hong Kong University of Science and technology, Clear Water Bay, Kowloon, Hong Kong, China*

(Received 2 August 2012; accepted 18 October 2012; published online 6 November 2012)

The dynamics of a 2D rotating Crookes radiometer is studied using a moving mesh unified gas kinetic scheme. The whole evolution process of a fan from an initial unsteady start-up to a final steady state rotational movement in a rarefied gas environment is simulated numerically. Through the numerical study, the unsteady force distribution along a vane which dynamically drives the fan movement is captured. And a quantitative connection between total torque and rotational speed of the fan in the Knudsen number regime of $10^{-3} < Kn < 10^{2}$ is obtained. Based on the dimensional analysis, the total radiometric torque can be decomposed into a net radiometric driving torque and a rotational resistance. Based on the numerical data, the analytical functions of the torque and angular velocity of a rotating fan in terms of Knudsen number are quantitatively constructed. This relationship is used to explain the experimental observation of the Knudsen number shift for the appearance of the maximum torque and the maximum rotational speed in the transitional flow regime. © *2012 American Institute of Physics*. [http://dx.doi.org/10.1063/1.4765353]

The Crookes radiometer[1] consists of a sealed glass bulb which is evacuated to a partial vacuum and a set of vanes mounted inside the bulb. The vanes are blackened on one side, and kept glossy on the other side. When exposed to light, the radiometer rotates. This interesting apparatus has attracted many renowned scientists' interests, such as Reynolds,[2,3] Maxwell,[4] and Einstein.[5] The driving force of Crookes radiometer, named radiometric force, has been identified. In the range of pressures for the maximum radiometric force,[6] both forces generated from the area and edge effect are important.[7] The area effect corresponds to the pressure difference between the two surfaces of the vanes in free molecular flow. And the edge effect corresponds to the well-known thermal transpiration near the edge of the vanes. In 1986, Binnig *et al.*[8] proposed the conception of atomic force microscope which employs microcantilever as a probe. This work encouraged the investigations of the Knudsen force in the transitional regime. For example, Passian *et al.*[9–11] studied the radiometric phenomena experimentally and analytically in application to microcantilevers. In recent years, a great effort has been made to get a better understanding of the radiometric force,[12–17] and many theories have been advanced to depict the radiometric force in the transitional regime. However, as shown by Selden *et al.*,[18] most of these theories are valid only in a small range of Knudsen number. It is hard to identify any preferred theory here.

Although plenty of studies have been made to explain the Crookes radiometer, there are few works targeting on the study of dynamical process of an unsteady freely rotating motion. After the discovery of the peak of radiometric force by Westphal,[6] Ota *et al.*[19] reported that, in the transitional regime, there was a shift between the maximum torque and maximum rotational speed in terms of Knudsen numbers in their experiment. This phenomenon indicates that the situation of a rotating vane differs from a static one. For a moving fan, Anikin[20] simulated the radiometric force of a 2D vane in a non-inertia rotational reference frame which is fixed on the vane. This is the first time

a)Electronic mail: cblee@mech.pku.edu.cn.

that a moving vane with a given constant angular velocity is considered numerically. He found that the total radiometric force is a linear function of the angular velocity of the vane. However, this methodology requires a constant rotation of the reference frame. As a result, it does not provide the dynamical acceleration process of the fan.

With the consideration of all these facts, in this work a unsteady start-up rotating fan will be investigated dynamically by numerical simulations. Based on the numerical solution and theoretical analysis, we are going to figure out the different kind of contribution of radiometric force in the static and rotating cases, which can be used to interpret the peak shift between the torque and angular velocity in terms of Knudsen numbers. A formula is derived to depict the total radiometric force for a wide range of Knudsen number.

The kinetic equation is solved by the unified gas kinetic scheme with a moving mesh[21–24] in this study. A cross shaped fan mounted in the center of a computational domain. The outside boundary is a circle with a radius of 0.2 m, which is twice of the length of the vane. The thickness of the vane is 0.01m. The rotational moment of inertia of the fan is 4.9×10^{-9} kg m^2. And the fan can rotate freely with a mechanical rotational resistance. The gas simulated here is argon with Pr = 2/3, and viscosity coefficient $\mu \sim T^{0.68}$. Because the glass bulb is transparent in the experiment, the light heats the vanes directly. As a result, the temperature in the center is larger than that at glass bulb. The two different coated sides of vanes also make different temperatures. Since this study does not examine temperature dependence of the system, the temperatures are set as constants. Specifically, the outside boundary is a solid fixed wall with a constant temperature of 300 K. The temperature at one side of each vane has a value of 350 K, and the other side keeps at 400 K. The temperature distribution at the lateral side of the vanes changes continuously from 400 K to 350 K. The topic of thermal variations on the radiometric forces is discussed by Lereu *et al.*[25] and Nabeth *et al.*[16] The diffusive boundary condition with fully accommodation coefficient is used at all solid boundaries. Considering a vane without thickness can generate radiometric force in Knudsen regime,[14] the Knudsen number in the current study is defined by the molecular mean free path over the length of the vane. And it varies from 0.001 to 10 which covers a wide range of flow regime from continuum flow to nearly free molecular one. The numerical experiments include two kinds of fan movements. The first one is a stationary case with a vanishing angular velocity $\omega = 0$, which is equivalent to the case with a large magnitude of mechanical friction. The second case is an idling case with a freely rotational movement and the neglect of mechanical friction of the rotor.

Figure 1 shows a typical temperature field at Kn = 0.1 for an idling moving fan after settling down to a steady state. The red parts present the high temperature areas. Owing to the higher temperature on the black surfaces induced by radiation heating, the molecules colliding with the hot black side leave with an increased velocity, exert a larger momentum on the black side than that on the white side, and consequently drive the vanes rotating counterclockwise. All the streamlines in Figure 1 are drawn from the absolute flow velocity in a laboratory inertia reference of frame. For a fixed fan, due to the thermal transpiration effect, the gas moves from the cold to the hot surfaces, and forms a circulation around the fan.[13,17] In present study, the circulation for a fixed fan is clockwise, and the torque exerted on the fan is in counterclockwise direction. But in this figure, the outside circulation is not obvious. In fact, for an idling moving fan at steady state, the total torque on the fan should be zero. Therefore, the reverse torque exerted on the gases should be zero as well. So is the torque on the gases from outside through the solid wall. As shown in Figure 1, there are several circulations in the domain. The sum of all these circulations should be constant. However, along the outside boundary, the circumferential velocity cannot be in a single direction. In another words, the gases cannot rotate all in the same direction near the outside boundary. Otherwise, a net torque which induced by directional tangential force will exert on the gases from the solid wall, which will not satisfy the steady state assumption for idling cases. As a result, for idling case, the gases cannot form a whole directional circulation at steady state in the laboratory inertia reference of frame.

The torque exerted on the vane can be decomposed into four parts, namely, the torques induced by the pressure and shear stress on the long arms and the lateral sides, which are represented by the symbols $M_{p,l}$, $M_{s,l}$, $M_{p,t}$, and $M_{s,t}$ respectively. As shown in the Table I, for the fixed vane case, the pressure torque on the long arm ($M_{p,l}$) is the greatest part among all the four torque sources, and is the only part with propulsive contribution. This observation is consistent with the simulation results

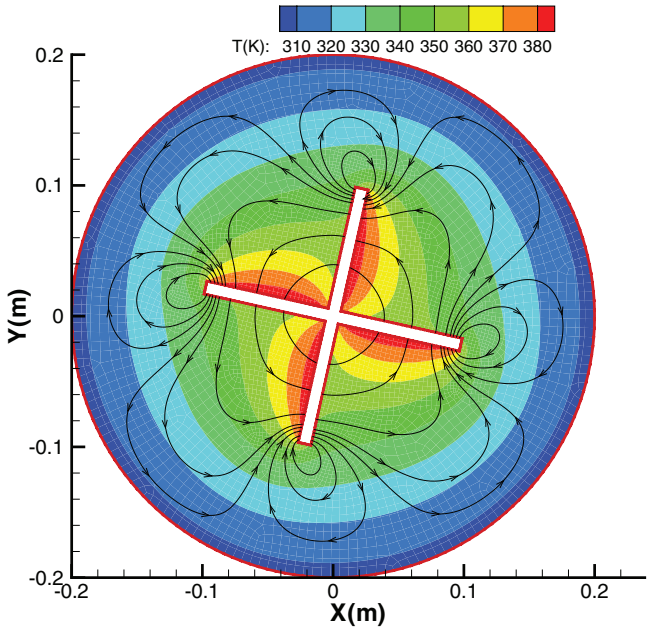

FIG. 1. The contours of Temperature field and the streamlines in laboratory inertia reference of frame at Kn = 0.1 for an idling moving fan.

reported in Refs. 18 and 26. For an idling fan, after settling down to a steady state with constant rotational speed, the total torque on the vane should be zero. Due to the symmetry of the fan, the torque exerted on each vane should be zero too. The Table I shows that, for an idling vane case, the torque $M_{p,l}$, which is induced by the pressure difference between the hot and cold sides along the long arms, decreases the most in comparison with the pressure torque in a fixed vane case. The pressure torque $M_{p,l}$ almost balances itself. Meanwhile the torques from the other sources keep the same order of magnitude as in the fixed vane case. It indicates that, for the idling moving vane, the final zero torque is mainly maintained by the redistribution of the gas pressure on the long arm.

Figure 2 shows a time-dependent variation of the pressure torque along the long arm in the initial starting movement phase of a rotating vane. The extent of the long arm is from 0.05 to 0.1. As shown in the figure, the initial pressure torque distribution is a straight line due to the constant pressure difference between the hot and cold sides along the long arm. Owing to the great pressure difference, the gases respond and get to a quasi-steady state quickly. At $t = 7 \times 10^{-4}$s, the angular velocity ω is still small, and the torque distribution is similar to that of a fixed fan, which is represented by a diamond line in Figure 2. As the fan rotates and gets a high angular velocity, the fan's tip velocity gets much higher than that in the center region. Then, the vane tip starts to push the surrounding gas away more efficiently. As a result, the pressure on the leading edge (cold side) near the tip becomes higher than that on the hot side. As shown by the line at $t = 3.1 \times 10^{-3}$s, the pressure difference reverses its sign from positive to negative near the tip of the vane. Therefore, the pressure torque near the tip will resist the fan's rotation. So, the acceleration of the angular velocity decreases gradually. When the positive part gets balanced with the negative part, which is represented by circle line in Figure 2, the fan settles to a steady state rotation. By examining all torques on the vane, the pressure

TABLE I. The torque induced by pressure and shear stress on a single vane for Kn = 0.1.

	$M_{p,l}$	$M_{s,l}$	$M_{p,t}$	$M_{s,t}$	M_{total}
Fixed (N · m)	1.830×10^{-5}	-1.172×10^{-6}	-1.568×10^{-7}	-1.074×10^{-6}	1.590×10^{-5}
Idling (N · m)	3.738×10^{-6}	-1.009×10^{-6}	-1.648×10^{-7}	-2.560×10^{-6}	4.262×10^{-9}

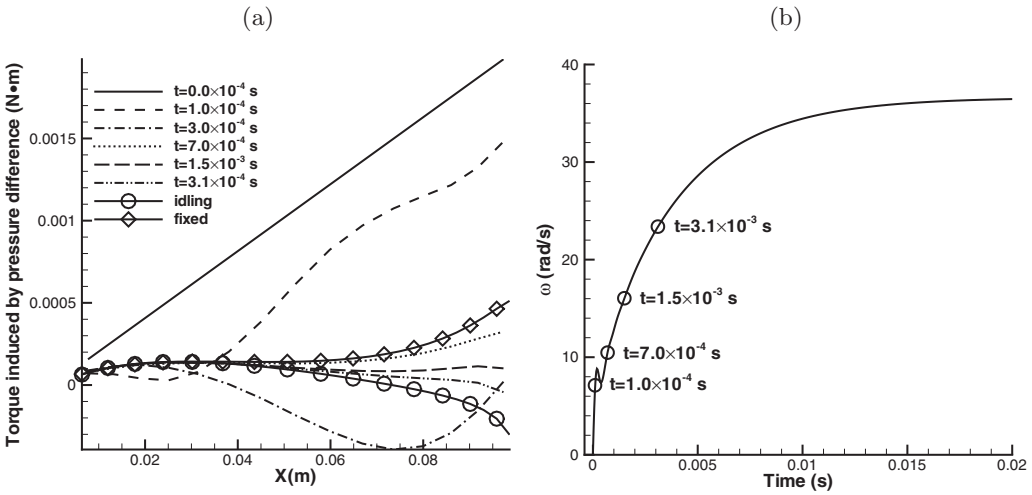

FIG. 2. The time series of the torque distribution along the long arm for Kn = 0.1.

torque generated near the center of the fan along the long arm is the only propulsive part. All other ones act oppositely. In this case, the force near the tip within one mean free path provides resistance for the fan movement. It is basically balanced by inner contributions of the vane. Therefore, the role played by the edge effect near the tip is different in the idling and the fixed fan cases. This dynamical torque evolution has not been identified before.

This kind of rotational resistance was first investigated by Anikin.[20] When the fan is forced to move with a constant angular velocity, based on the steady state flow field around the fan, the total torque from the gas can be calculated. Under this condition, Anikin discovered a linear relationship between the rotational rate of the fan and the total radiometric torque.[20] Through our numerical study, we obtained similar results for many other Knudsen numbers. Figure 3 presents many cases over a wide range of Knudsen numbers, i.e., Kn = 0.001 ∼ 10. The intersection of each line with the torque axis corresponds to the fixed fan cases. Among these lines, the maximum torque has a value of 6.3×10^{-5}N m, which corresponds to a Knudsen number around 0.1. The interception of the curves on the angular velocity axis corresponds to the idling fan case. The maximum of angular

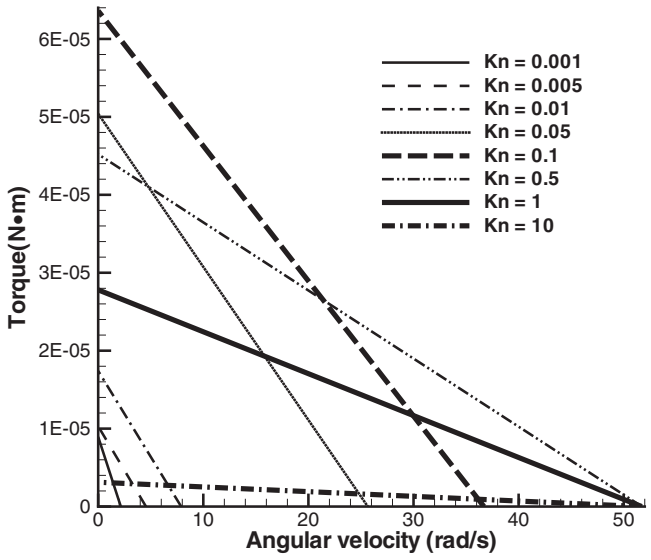

FIG. 3. The total radiometric torque versus rotational rate under different Knudsen numbers.

velocity ω is about 51.7rad/s, which appears at a Knudsen number between 0.5 and 1. The three lines at Kn = 0.01, 0.1, 0.5 in the current calculations are close to the results at Kn = 1/12, 1/5, 1/2 in Ref. 20. These differences are due to the different setup of the numerical experiments.

Besides the numerical simulation of the Crookes radiometer, we are going to perform dimensional analysis to get a deep insight for Crookes radiometer. Similar works have been done for fixed vane or microbeam by Taguchi *et al.*[14] and Nabeth *et al.*[16] A formula will be derived to depict the relationship among the total torque, the angular velocity, and the Knudsen numbers. With this formula, the peak shift phenomenon can be derived quantitatively.

The physical quantities influencing the radiometer performance are chosen as follows:

$$(R\Delta T, \rho, l, p, D, M, \omega).$$

Here, a 2D fan sitting in an infinite space with length D is considered. The parameter l represents the mean free path of ambient gas. ρ is the density, and p is the pressure. M denotes the torque at steady state rotation with a constant angular velocity ω. R is the gas constant, and ΔT represents the temperature difference. The ideal gas relation is employed here. After dimensional analysis, we can get four dimensionless quantities,

$$\pi_1 = \left(\frac{p}{\rho R\Delta T}\right) = \frac{T}{\Delta T}, \tag{1}$$

$$\pi_2 = \frac{l}{D}, \tag{2}$$

$$\pi_3 = (R\Delta T)^{-1}\rho^{-1}l^{-2}M, \tag{3}$$

$$\pi_4 = (R\Delta T)^{-1}l^2\omega^2. \tag{4}$$

The first one is the ratio of heating temperature ΔT to the ambient temperature T. The second one is Knudsen number. Based on the numerical observation in Figure 3 that the torque M is a linear function of ω, the relation between the π_3 and π_4 will take the following form:

$$\pi_3 = \pi_4^{\frac{1}{2}} C_1^*(\pi_1, \pi_2) + C_2^*(\pi_1, \pi_2). \tag{5}$$

Then,

$$M = \rho D^3\sqrt{R\Delta T}\omega C_1\left(\frac{\Delta T}{T}, \mathrm{Kn}\right) + pD^2 C_2\left(\frac{\Delta T}{T}, \mathrm{Kn}\right). \tag{6}$$

Here, the parameters C_1 and C_2 are unknown functions of $T/\Delta T$ and Kn. Conventionally, C_1 is called rotational resistance coefficient, and C_2 is called net radiometric torque coefficient.

The computed lines in Figure 3 are matched by a straight line, $M = \alpha\omega + \beta$, where α and β only depend on the Knudsen number here. The values of α and β in all simulation cases at different Kn can be obtained. Define new variables of $\tilde{\alpha} = \alpha/(\rho D^3\sqrt{R\Delta T})$ and $\tilde{\beta} = \beta/(pD^2)$. Then, we can get the numerical experimental data as $M_{num} = \rho D^3\sqrt{R\Delta T}\tilde{\alpha}\omega + pD^2\tilde{\beta}$. By fitting the numerical data by curves versus Knudsen number, we can get an analytic formulation for C_1 and C_2. The fitting function for C_1 and C_2 takes the following form:

$$C_{1,2} = \eta_1 \tanh(\eta_2 \lg(\mathrm{Kn}) + \eta_3) + \eta_4, \tag{7}$$

TABLE II. Detailed value for the rotational resistance coefficient and the net radiometric torque coefficient.

	η_1	η_2	η_3	η_4
For C_1	−1.57571	1.18743	0.64549	−1.58233
For C_2	0.03002	1.60692	0.90533	0.03002

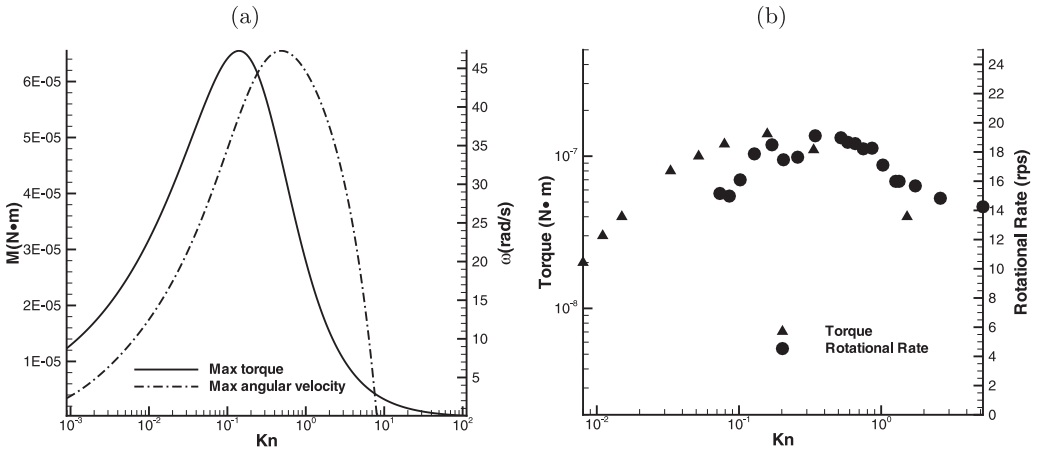

FIG. 4. The peak shift between the curve of the total torque and the curve of the angular velocity vs. Knudsen numbers. (a) The fitting data from current numerical simulation. (b) The experimental data for argon extracted from Ref. 19.

where $\eta_{1,2,3,4}$ are constants. It should be noted that the formulations for the C_1 and C_2 are identical. Actually, some other force coefficients in terms of Knudsen number, such as the drag coefficient of flow past cylinder[27] and the Knudsen force coefficient on a flat plate,[14] can be fitted well by this formula. Considering no radiometric force exerted on the vane in continuum flow limit, the fitting coefficients η_4 will be equal to η_1 in the determination of net radiometric torque coefficient C_2. The specific values of $\eta_{1,2,3,4}$ can be fully determined and listed in Table II.

For a general case in the laboratory experiment, the mechanical friction must be taken into consideration. Here, assuming a sliding friction of $M_{rotor} = 4 \times 10^{-6}$N m, let the total radiometric torque M balance with M_{rotor}. The corresponding curves for maximum angular velocity, namely, $\omega = (M_{rotor} - pD^2C_2(\mathrm{Kn}))/(\rho D^3\sqrt{R\Delta T}\omega C_1(\mathrm{Kn}))$, is derived. In Eq. (6), assuming $\omega = 0$, the curve for maximum torque under fixed cases is presented by function $M = pD^2C_2(\mathrm{Kn})$. These two curves are plotted in Figure 4. Under these conditions, the maximum total torque appears at about $\mathrm{Kn} = 0.14$ and the maximum angular velocity arises at about $\mathrm{Kn} = 0.48$. These results are consistent with the experimental observation in Ref. 19, which is presented in Figure 4 as well. The reason for the shift of maximum values is due to the two different kinds of radiometric torque in the fixed and rotational cases from the edge effect. As illustrated in Figure 2, for a fixed fan or at the very initial stage of a rotating fan, due to the thermal transpiration, the pressure torque around the tip area is positive and intends to rotate the fan. However, as an increasing of angular velocity, the torque contribution around the tip region becomes resistance. Apparently, these two kinds of edge effect corresponding to different radiometric torque act differently when the Knudsen number changes.

In present study, the whole dynamic process of a moving Crookes radiometer is simulated from an initial start-up to a final steady state rotation. The rotational behavior is determined both by the net radiometric torque and the rotational resistance. Through the dimensional analysis and the use of the simulation data, two coefficients, namely, the rotational resistance coefficient and the net radiometric torque coefficient, are fully determined. These two coefficients have a similar functional dependence on the Knudsen number, which connects the continuum flow limit to the free molecular motion. The formulation obtained in this study can be used to explain the experimental measurements conducted in a wide range of Knudsen numbers.

This work was supported by the National Natural Science Foundation of China under Grant No. 10087101, National Natural Science Foundation of China (Project No. 10772033), Hong Kong Research Grant Council (621709, 621011), and grants SRFI11SC05 and RPC10SC11 from HKUST.

[1] W. Crookes, "On attraction and repulsion resulting from radiation," Philos. Trans. R. Soc. London **164**, 501–527 (1874).
[2] O. Reynolds, "On the forces caused by the communication of heat between a surface and a gas; and on a new photometer," Philos. Trans. R. Soc. London **166**, 725–735 (1876).

[3] O. Reynolds, "On certain dimensional properties of matter in the gaseous state," Philos. Trans. R. Soc. London **170**, 727–845 (1879).
[4] J. C. Maxwell, "On stresses in rarefied gases arising from inequalities of temperature," Philos. Trans. R. Soc. London **170**, 231–256 (1879).
[5] A. Einstein, "Zur theorie der radiometerkräfte," Z. Phys. **27**, 1–6 (1924).
[6] W. H. Westphal, "Messungen am radiometer," Z. Phys. **1**, 92–100 (1920).
[7] N. Selden, C. Ngalande, S. Gimelshein, E. P. Muntz, A. Alexeenko, and A. Ketsdever, "Area and edge effects in radiometric forces," Phys. Rev. E **79**, 041201 (2009).
[8] G. Binnig, C. F. Quate, and C. Gerber, "Atomic force microscope," Phys. Rev. Lett. **56**, 930–933 (1986).
[9] A. Passian, A. Wig, F. Meriaudeau, T. L. Ferrell, and T. Thundat, "Knudsen forces on microcantilevers," J. Appl. Phys. **92**, 6326 (2002).
[10] A. Passian, R. J. Warmack, A. Wig, R. H. Farahi, F. Meriaudeau, T. L. Ferrell, and T. Thundat, "Observation of Knudsen effect with microcantilevers," Ultramicroscopy **97**, 401–406 (2003).
[11] A. Passian, R. J. Warmack, T. L. Ferrell, and T. Thundat, "Thermal transpiration at the microscale: A Crookes cantilever," Phys. Rev. Lett. **90**, 124503 (2003).
[12] M. Scandurra, F. Iacopetti, and P. Colona, "Gas kinetic forces on thin plates in the presence of thermal gradients," Phys. Rev. E **75**, 026308 (2007).
[13] L. H. Han, S. M. Wu, J. C. Condit, N. J. Kemp, T. E. Milner, M. D. Feldman, and S. C. Chen, "Light-powered micromotor driven by geometry-assisted, asymmetric photon-heating and subsequent gas convection," Appl. Phys. Lett. **96**, 213509 (2010).
[14] S. Taguchi and K. Aoki, "Numerical analysis of rarefied gas flow induced around a flat plate with a single heated side," AIP Conf. Proc. **1333**, 790–795 (2011).
[15] T. S. Zhu and W. J. Ye, "Origin of Knudsen forces on heated microbeams," Phys. Rev. E **82**, 036308 (2010).
[16] J. Nabeth, S. Chigullapalli, and A. A. Alexeenko, "Quantifying the Knudsen force on heated microbeams: A compact model and direct comparison with measurements," Phys. Rev. E **83**, 066306 (2011).
[17] Y. A. Anikin, "Numerical study of radiometric forces via the direct solution of the Boltzmann kinetic equation," Comput. Math. Math. Phys. **51**, 1251–1266 (2011).
[18] N. Selden, C. Ngalande, N. Gimelshein, S. Gimelshein, and A. Ketsdever, "Origins of radiometric forces on a circular vane with a temperature gradient," J. Fluid Mech. **634**, 419–431 (2009).
[19] M. Ota, T. Nakao, and M. Sakamoto, "Numerical simulation of molecular motion around laser microengine blades," Math. Comput. Simul. **55**, 223–230 (2001).
[20] Y. A. Anikin, "Numerical study of the radiometric phenomenon exhibited by a rotating Crookes radiometer," Comput. Math. Math. Phys. **51**, 1923–1932 (2011).
[21] K. Xu and J. C. Huang, "A unified gas-kinetic scheme for continuum and rarefied flows," J. Comput. Phys. **229**, 7747–7764 (2010).
[22] K. Xu and J. C. Huang, "An improved unified gas-kinetic scheme and the study of shock structures," IMA J. Appl. Math. **76**, 698–711 (2011).
[23] J. C. Huang, K. Xu, and P. B. Yu, "A unified gas-kinetic scheme for continuum and rarefied flows II: Multi-dimensional cases," Comm. Comp. Phys. **12**, 662–690 (2012).
[24] S. Z. Chen, K. Xu, C. B. Lee, and Q. D. Cai, "A unified gas kinetic scheme with moving mesh and velocity space adaptation," J. Comput. Phys. **231**, 6643–6664 (2012).
[25] A. L. Lereu, A. Passian, R. J. Warmack, T. L. Ferrell, and T. Thundat, "Effect of thermal variations on the Knudsen forces in the transitional regime," Appl. Phys. Lett. **84**, 1013–1015 (2004).
[26] N. E. Gimelshein, S. F. Gimelshein, A. D. Ketsdever, and N. P. Selden, "Shear force in radiometric flows," AIP Conf. Proc. **1333**, 661–666 (2011).
[27] G. J. Maslach and S. A. Schaaf, "Cylinder drag in the transition from continuum to free molecule flow," Phys. Fluids **6**, 315 (1963).